Quantification of Redox-Induced Thickness Changes of 11-Ferrocenylundecanethiol Self-Assembled Monolayers by Electrochemical Surface Plasmon Resonance

Xin Yao,[†] Jianxiu Wang,[†] Feimeng Zhou,*[,†,‡] Jun Wang,[‡] and Nongjian Tao[§]

Department of Chemistry, Graduate School, Chinese Academy of Science, Beijing 100039, P.R. China, Department of Chemistry and Biochemistry, California State University, Los Angeles, Los Angeles, California 90032, and Department of Electrical Engineering, Arizona State University, Tempe, Arizona 85287

Received: January 24, 2004; In Final Form: March 17, 2004

Redox-induced orientation changes (or monolayer thickness changes) of self-assembled monolayers (SAMs) of 11-ferrocenylundecanethiol ($FcC_{11}SH$) were quantified by the electrochemical surface plasmon resonance (EC−SPR). EC−SPR enables one to determine the collective effect of the monolayer thickness and refractive index changes resulted from the oxidation of ferrocene (Fc) to ferrocenium. To measure the monolayer volume variation associated with the molecular orientation change, an electrochemical quartz crystal microbalance (EQCM) was used to determine the total number of water molecules accompanying with the ion-pairing between the ferrocenium cation and the counteranion in the solution. With the maximum void space within the SAM for water incorporation known, the Lorentz−Lorenz equation was used to correlate the SPR dip shift to the maximum monolayer thickness variation. In the presence of 0.1 M $HClO_4$ and 0.1 M HNO_3, the monolayer thickness changes were deduced to be 0.09 and 0.08 nm, respectively. Thus, upon electrochemical oxidation of the $FcC_{11}SH$ SAM, the swinging of the alkyl chain farther away from the electrode (Ye et al., *Langmuir*, **1997**, *13*, 3157) or the rotation or flipping of the Fc cyclopentyldiene ring around the bond between the Fc group and the alkyl chain (Viana et al., *J. Electroanal. Chem.* **2001**, *500*, 290) can both lead to the observed film thickness changes, with the former probably being the more important process.

1. Introduction

Self-assembled monolayers (SAMs) of alkanethiols or alkanethiols bearing different functional groups[1−4] (e.g., electroactive[5−20] or photoactive[21,22] moieties) have been routinely employed as model systems for probing interfacial phenomena, such as electron transfer (ET),[19,23−39] lubrication,[40] biomolecular adsorption and cross-linking reactions,[41−47] and heterogeneous catalysis.[48−51] Alkanethiol SAMs terminated with electroactive groups have received a great deal of attention, owing to the intricate relationship between the ET rate and a variety of surface and solution parameters. These parameters include, but are not limited to, coverage, orientation, and chain length of the alkanethiol molecules containing electroactive termini, the nature of another alkanethiol in a mixed SAM, and the electrolyte system in which heterogeneous ET reactions take place. It is also well known that, when redox reactions of the terminal groups create or annihilate charges at the monolayer/solution interface, formation or dissociation of ion pairs may occur.[15,28,52−56] Such a process is frequently accompanied by the orientation/structural change of the alkanethiol molecules (redox-induced orientation change[15,20,55−60]). For example, using electrochemical quartz crystal microbalance (EQCM), De Long and Buttry found that methyl viologen groups situated at the solution termini of an alkanethiol SAM, upon reductions, would result in mass losses that are indicative of the dissociation of ion pairs.[52] Uosaki and co-workers, utilizing a wide range of surface techniques, have systematically characterized the redox-induced orientation change of ferrocene (Fc)-terminated alkanethiol SAMs.[55,56,60] Concerning such an orientation change, on the basis of in-situ infrared reflection absorption spectral peaks, these researchers suggested that the tilt angle of the alkyl chain would decrease with respect to the surface normal as the Fc groups become oxidized to the positively charged ferrocenium cations.[55] Alleviating the electrostatic repulsion among the adjacent ferrocenium cations and that between the ferrocenium cations and the positively charged electrode is reasoned for such a reorientation. Viana et al. carried out a similar voltammetric and infrared spectroscopic study but concluded that, instead of decreasing the tilt angle, the cyclopentyldiene (Cp) ring of the Fc molecule would flip around the Fc-C bond at the end of the SAM.[53] For comparison, the schemes of these two different mechanisms are reproduced in Figure 1. As contrasted by the two mechanisms, swing of the alkyl chain (Figure 1a) toward the surface normal should cause a different change in the SAM thickness than the flipping of the Cp ring (Figure 1b). In either case, the change of the SAM thickness is expected to be in the sub-nanometer range. Interestingly, such a tiny change has been shown to be capable of triggering a drastic switch of liquid crystals at surfaces.[20] Thus, an accurate determination of the film thickness change will not only help clarify the surface process(es) accompanying the electrochemical oxidation of the Fc groups but also can shed light on the parameters governing device performance. Uosaki and co-workers have used in-situ ellipsometry to determine the redox-induced orientation change of such SAMs.[60] Unfortunately, the accuracy is largely compromised by the low signal-to-noise ratios. In fact, multiple ellipsometric scans had to be performed

* Corresponding author. Tel: 323-343-2390. Fax: 323-343-6490. Email: fzhou@calstatela.edu.
[†] Chinese Academy of Science.
[‡] California State University, Los Angeles.
[§] Arizona State University.

10.1021/jp049651y CCC: $27.50
Published on Web 04/30/2004

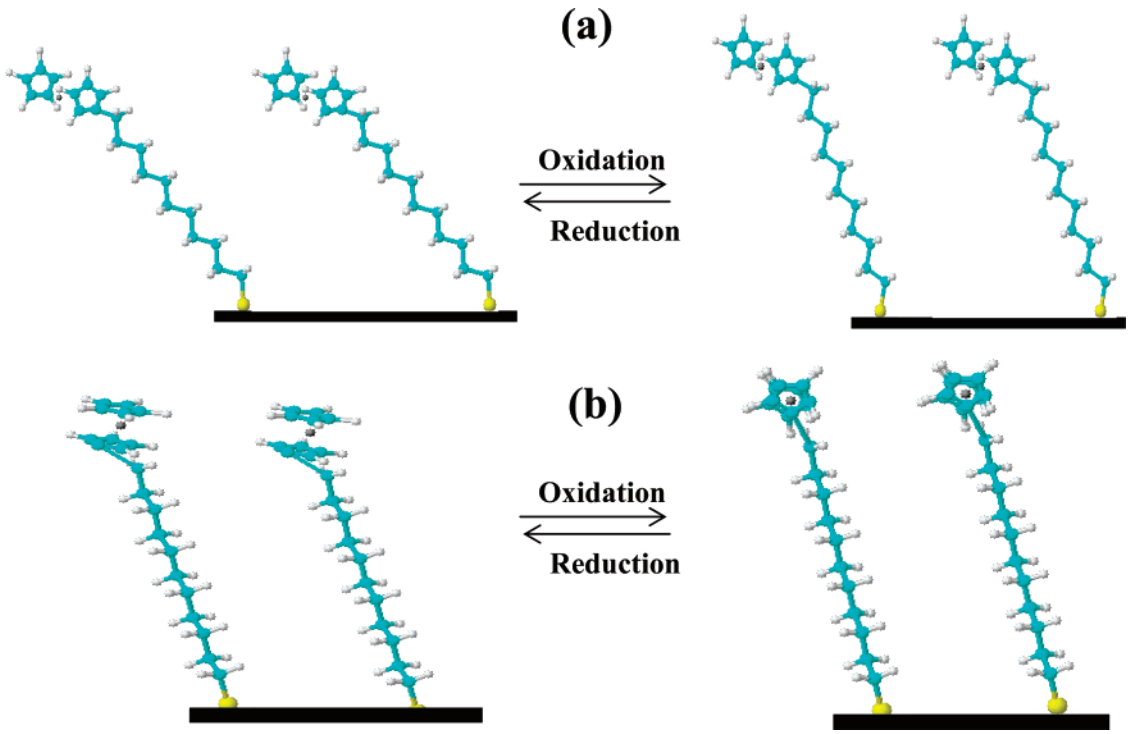

Figure 1. Schematic representation of the two mechanisms accounting for the orientation change of the 11-ferrocenylundecanethiol SAM accompanying the Fc oxidation and the subsequent ion-pairing process. In (a), charging of the electrode surface and conversion of Fc to ferrocenium ions leads to a decrease in the tilt angle of the alkanethiol chain. For clarity, insertion of water molecules into the monolayers is not shown. In (b), upon Fc oxidation, the Fc group rotates from a tilted conformation to a position wherein the cyclopentyldiene rings become perpendicular to the electrode.

and averaged. To fully understand the extent of molecular reorientation, it is evident that one must resort to a technique that can reliably determine the monolayer thickness variation at a sensitive level.

In recent years, surface plasmon resonance (SPR) and its combination with electrochemistry (EC−SPR) have emerged as powerful tools for probing extremely small changes of various adsorbate films at the metal/solution interface.[10,61−65] We have recently developed a high-resolution surface plasmon resonance (SPR) spectrometer and combined it either with electrochemistry for the study of conformational and electronic changes of redox proteins[66] or with flow injection analysis for ultrasensitive detection of DNA hybridization reactions.[67] As little as 0.05 nm was easily detected by EC−SPR for the redox-induced cytochrome *c* monolayer film thickness change.[66] Moreover, attomole quantities of oligonucleotides adsorbed onto surfaces can be quantified.[67] Such a remarkable sensitivity to adsorbate structural change or surface adsorption is attributable to the utilization of a bicell detector that can measure infinitesimal variation of the SPR dip shift. Since the orientation change caused by the oxidation of the terminal Fc groups of the SAMs is expected to be only in the sub-nanometer range,[8,53,55,60] the advantage of using such a highly sensitive SPR becomes apparent. In this work, we show that thickness changes of FcC_{11}-SH SAMs in the presence of different electrolytes can be accurately measured by EC−SPR. EQCM results confirm that water molecules are brought onto and/or into the $FcC_{11}SH$ SAM upon the Fc oxidation. The maximum change of refractive index of the SAM caused by the monolayer volume variation and water incorporation can be gauged by performing a calculation based on the Lorentz−Lorenz equation using the void space within the $FcC_{11}SH$ SAM for the water incorporation. As recently shown by Plunkett et al.,[68] the use of QCM and SPR in parallel provides an opportunity to gain a better understanding of adsorption processes. EQCM is sensitive to the mass change of adsorbates oscillating with the crystal, together with the hydrodynamically coupled solvent molecules, whereas the SPR technique measures the difference in the refractive indexes that are only affected by the solvent molecules entrapped inside adsorbate films. We show that the tandem use of EC−SPR and EQCM is an attractive approach for delineating the various redox-triggered surface processes of $FcC_{11}SH$ SAMs.

2. Experimental Section

2.1. Chemicals. 11-Ferrocenylundecanethiol ($FcC_{11}SH$) was purchased from Dojindo Co. (Atlanta, GA). Perchloric acid, nitric acid, and hexane (Beijing Reagent Co.) were of reagent grade and used without further purification. All electrolyte solutions were prepared with water treated by a purification system (Simplicity Plus, Millipore Inc.). Fc was obtained from Aldrich and ferrocenium hexafluorophosphate was kindly provided by Prof. B. T. Donovan-Merkert (University of North Carolina−Charlotte).

2.2. Electrodes and Cells. BK7 glass slides (Fisher) were thoroughly rinsed with acetone, ethanol, and water. Upon drying, 50-nm-thick gold films with 2 nm Cr underlayers were deposited using a sputter coater (model 108, Kert J. Lester Inc., Clairton, PA). The QCM crystals (5 mm in diameter, ICM Technologies, Oklahoma City, OK) were AT-cut and had a fundamental frequency of 9.995 MHz. The gold-coated glass slides or quartz crystals were modified with $FcC_{11}SH$ SAMs and became part of a one-compartment cell. A Ag/AgCl and a platinum wire were used as the reference and auxiliary electrodes, respectively. To avoid potential chloride ion contamination, the reference electrode was separated from the electrochemical cell by a salt bridge containing saturated KNO_3. To measure the SPR dip shifts as a function of the applied potential, seven replicates were carried out at different $FcC_{11}SH$ SAM-modified gold films in both $HClO_4$ and HNO_3 solutions and the averaged SPR dip

shift values were used to compute the film thickness variations accompanying the potential scans.

2.3. Instruments. EQCM measurements were conducted with a CHI 440 electrochemical workstation (CH Instruments, Austin, TX). The homemade EQCM cell[69] and the oscillator box were housed in a Faraday cage. The EC−SPR setup is similar to that previously reported.[65,66] Two diode lasers, with respective emission wavelengths at 675 and 785 nm, were used in conjunction with a LDC 500 laser driver (Thorlabs, Newton, NJ). A CHI 610 electrochemical analyzer was employed for the cyclic voltammetric experiments, while the SPR signals were recorded with a digital oscilloscope (Yokogawa, model DL1520L). Our high-resolution SPR instrument measures reflected light at two photodetectors (A and B) of a bicell and the SPR dip shift is proportional to the ratio of (A−B)/(A+B). To convert the ratio of (A−B)/(A+B) to the SPR dip shift, we carried out a calibration experiment by gradually adding predetermined amounts of ethanol into pure water and measuring the corresponding SPR signal. By comparing the slope of the resultant linear plot of (A−B)/(A+B) against the ethanol content to that of the curve computed by Kolomenskii et al.,[70] 1.06 was determined to be the proportionality constant. Since there is no adsorption occurring upon the addition of ethanol to water and changes of the SPR dip shifts measured by this work are small, the SPR dip shifts should be approximately proportional to the changes of refractive index of the solution. The proportionality would vary depending on the specific instrument design and the types of substrates used. Thus, by comparing the experimentally measured SPR dip shift−refractive index relationship to that in the paper by Kolomenskii,[70] the instrument can be calibrated. We have also compared such a calibration to the measurements using a CCD detector[65] and found that both methods yielded essentially the same calibration curve. Refractive indices of HNO_3 and $HClO_4$ solutions of different concentrations were measured with an Abbe refractometer (model FOIC, Guizhou Xintian High-Precision Optics Inc., China).

2.4. Preparation of $FcC_{11}SH$ SAM-Modified Gold Substrates. The gold-coated glass slide was briefly annealed in a hydrogen flame before each experiment to reduce surface contamination. The annealed gold film was immediately dipped in a hexane solution containing 0.4 mM $FcC_{11}SH$ for 12 h. This step was followed by rinsing with copious amounts of hexane and water and drying under a stream of N_2. The QCM crystal was cleaned with a piranha solution (30% H_2O_2 and 70% concentrated H_2SO_4). Rinsing, drying, and modifying the crystals with $FcC_{11}SH$ followed the procedure for modifying the SPR substrate.

3. Results and Discussion

Before we present our EC−SPR data, it is necessary to review results from various electrochemical, spectroscopic, and microgravimetric characterizations of Fc-terminated SAMs.[2,8,14−16,24,25,27,34,38,39,53−58,60,71,72] The point of zero charge of a SAM-modified gold electrode is about −0.4 V vs Ag/AgCl.[26] As a result, within the potential range where Fc moieties are oxidized (typically from 0.2 to 0.8 V vs Ag/AgCl), the electrode surface is positively charged. In the first mechanism (Figure 1a), it is generally believed that oxidation of Fc to ferrocenium introduces two kinds of electrostatic repulsions, viz., that between two adjacent ferrocenium cations and that between the positively charged electrode and the ferrocenium cation. To counterbalance the electrogenerated ferrocenium ions, anions in the solution would form ion pairs at the end of the SAM.[34,55−60] The ion pairing has been confirmed by EQCM experiments and elemental analysis.[28,34,48,52,56,58,59,72−74] Moreover, to further offset the electrostatic repulsion between the ferrocenium ions and the electrode, the tilt angle of the alkyl chain with respect to the surface normal would decrease. Such an orientation change is supported by FT-infrared reflection absorption spectroscopy[55] and ellipsometry.[60] Uosaki and coworkers also suggested that the increase of hydrophilic property of the monolayer after the oxidation of the terminal Fc moiety should enhance the incorporation of water and anions, and the extent of the water loading depends on the nature of the anion and the surface coverage of the Fc-terminated SAMs.[56,58,59] In the second mechanism (Figure 1b), based on subtractively normalized interfacial FT-IR spectroscopy results, Viana et al. postulated that rotation/flipping of the Fc group around the alkyl chain would occur.[53] From the intensity of the IR bands of the intrinsic carbonyl groups in the Fc-terminated alkanethiol compound used in their study, these researchers concluded that there exists no evidence for an appreciable change in the orientation of the alkyl chains.

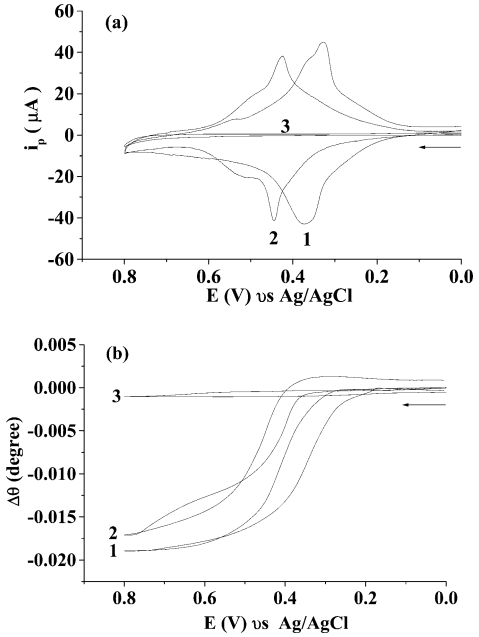

Figure 2. Cyclic voltammograms (panel a) of $FcC_{11}SH$ SAMs in 0.1 M $HClO_4$ (curve 1) and 0.1 M HNO_3 (curve 2) and the corresponding SPR dip shift-potential diagrams (panel b). Curves 3 in panels a and b correspond to the voltammogram of a hexanethiol SAM and the SPR dip shift potential diagram, respectively. Arrows indicate the scan direction and the scan rate was 50 mV/s.

Figure 2 is an overlay of cyclic voltammograms (CVs, panel a) of $FcC_{11}SH$ monolayers acquired from 0.1 M $HClO_4$ (curve 1) and 0.1 M HNO_3 (curve 2), together with the simultaneously recorded SPR dip shifts (panel b). Well-defined reversible redox waves were observed in both solutions. The broad shapes of and the presence of shoulder peaks in the voltammograms have been attributed to the existence of small structural disorders of ferrocenylalkanethiol SAMs of high surface coverage.[25] The peak potentials (Table 1) were found to be dependent on the nature of the anions in solution, a phenomenon that has been noted by several studies.[25,75] As shown in Table 1, the anodic peak current (i_{pa}) was essentially of the same magnitude as the cathodic peak current (i_{pc}). In addition, i_{pa} values were found to be proportional to the scan rates between 0.05 and 0.3 V/s. All these characteristics[76] confirmed that the surface-confined Fc groups could undergo facile ET reactions with the underlying electrode.[6,7,12−15,19,23−26,27,29,30,32,35,53,55−60,72,75,77] The surface coverage (Γ) values of the $FcC_{11}SH$ SAM were estimated by

TABLE 1: EC−SPR and EQCM Measurements

anion (0.1 M)	i_{pa}/i_{pc}	E_{pa} (V)	E_{pc} (V)	$\Delta\theta$ (degree)	Δf (Hz)	N_w/N_q	Δd (nm)
ClO_4^-	0.95	0.368	0.337	-0.0188 ± 0.0007	35	17 ± 3	0.09 ± 0.003
NO_3^-	1.07	0.450	0.418	-0.0176 ± 0.0019	55	35 ± 4	0.08 ± 0.009

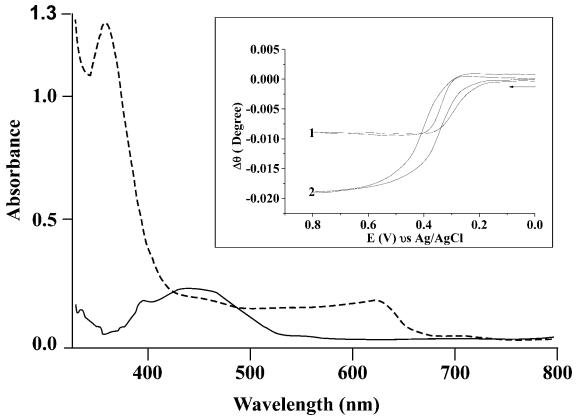

Figure 3. UV−visible spectra of 0.2 mM Fc (solid line curve) and 0.2 mM ferrocenium (dotted line curve) dissolved in hexane. SPR dip shift potential diagrams using two different laser diodes (curve 1 with the 675 nm diode laser and curve 2 with the 785 nm diode laser) are shown in the inset.

integrating the anodic peaks (2.3×10^{14} molecules/cm^2 in $HClO_4$ and 2.2×10^{14} molecules/cm^2 in HNO_3). These values are close to the maximum coverage of a typical ferrocenylalkanethiol SAM (2.7×10^{14} molecules/cm^2 [27,71]). The Γ values are reasonably high, suggesting that the as-prepared SAMs are quite compact and close to a full monolayer.

Perhaps the most noteworthy findings are the magnitudes of the SPR dip shifts (Table 1). As can be seen in Figure 2b, the shape of the SPR dip shift potential curves is sigmoidal and the onset of the SPR dip shift coincides with the oxidation wave of the $FcC_{11}SH$ SAM (Figure 2a). Note that the multiple measurements ($n = 7$) of the plateaus of the SPR curves yielded small standard deviations, suggesting that the experiments are quite reproducible. Two aspects are worth mentioning: (1) the change of the SPR dip is rather abrupt, suggesting that the redox-induced monolayer reorganization or film thickness change is instantaneous, and (2) the extent of the SPR dip shift is dependent on the counterion in the electrolyte solution to some extent. To exclude the possible influence of the SPR dip shift by the change in the electron density of the electrode during the potential scan,[66] we carried out an EC−SPR experiment at a gold electrode modified with a hexanethiol SAM. As shown by curve 3, when there are no electroactive groups at the end of the SAM, the change of the SPR dip shift in the anodic direction is nonsigmoidal and rather small (~0.001°), suggesting that the variation of the electron density of the underlying electrode would not cause an appreciable SPR dip shift.

Since ferrocenium cations and Fc molecules absorb in the different regions of the visible spectrum, it is possible that the absorption of either species contributed to the observed SPR dip shift. We therefore carried out UV−visible spectrometric measurements in hexane solutions comprising Fc or ferrocenium hexafluorophosphate to choose the appropriate incident light wavelength. As can be seen from Figure 3, the Fc solution displayed an absorption peak at 455 nm, whereas the ferrocenium hexafluorophosphate solution showed a peak at 622 nm. It is known that change of the refractive index (Δn) is negligible when the wavelength of the incident light (λ) is quite different than the absorption peak of the species at the surface.[66] Thus, the laser diode with the emission wavelength at 785 nm should be a good choice, because it is far away from both Fc and ferrocenium absorption peaks. When a diode laser that emits light at 675 nm (close to the tail end of the ferrocenium absorption peak) was used, the SPR dip shift was found to be much smaller than that obtained with a laser diode of 785 nm (inset of Figure 3). We should add that 785 nm is close to the infrared region and the laser spot is quite faint. Interestingly, the SPR dip shift (the dark line[65]) is even easier to distinguish, making the measurements quite reliable.

Thus, the SPR dip shift $\Delta\theta$ measures changes in both the refractive index (Δn) and the thickness (Δd) produced by the monolayer reorientation or reorganization:[66]

$$\Delta\theta = c_1\Delta n + c_2\Delta d \qquad (1)$$

where c_1 and c_2 are constants. The values of c_1 and c_2 were deduced to be 3.25 and 0.18 from numerical simulations based on Fresnel configuration containing four phases, a BK7 prism ($n = 1.515$), a gold film ($n = 1.26$ and $d = 50$ nm), the FcC_{11}-SH SAM ($n = 1.464$ and $d = 2.37$ nm[60]), and the electrolyte solution ($n = 1.33$). It is reported that the counteranions reside on top of the $FcC_{11}SH$ SAMs[55,58] and consequently a five-phase system could also be formulated in correlating the measured $\Delta\theta$ value with Δd. However, considering that the refractive indices of relatively dilute $HClO_4$ and HNO_3 do not deviate greatly from that of pure water, the effect of these counteranions should be negligible. Indeed, using the refractive indices measured from 0.1 M $HClO_4$ (1.3325) and 0.1 M HNO_3 (1.3328) and the diameters of ClO_4^- (4.72 Å) and NO_3^- (3.78 Å[78]), the SPR dip shifts deduced from the five-phase system differ from the four-phase counterparts by only 0.0002° and 0.0004° for $HClO_4$ and HNO_3, respectively. Thus, the additional anionic layer can be considered to be part of the solution medium. The thickness of the $FcC_{11}SH$ SAM was calculated by assuming a tilt angle of 27° with respect to the surface normal[27,33,71,79] and the $FcC_{11}SH$ chain length of 2.66 nm (i.e., the sum of the undecanethiol chain length, 2.0 nm,[27,60] and the diameter of a Fc sphere, 0.66 nm[27]). Such a value has also been used by other researchers.[60] In eq 1, upon monolayer oxidation, the $FcC_{11}SH$ molecular orientation change will not only alter the monolayer thickness d but also change the n value of the monolayer. The Lorentz−Lorenz relation suggests that the variation of n will be related to the total volume of the monolayer, V, which is the sum of the volumes occupied by the SAM molecules (V_f) and the associated water molecules (V_w):

$$\Delta n = -\frac{1}{6n}(n^2+2)^2\left(\frac{n^2-1}{n^2+2} - \frac{n_w^{\,2}-1}{n_w^{\,2}+2}\frac{V_f}{V}\right)\frac{\Delta d}{d} \qquad (2)$$

where n_w is the refractive index of water and d is the thickness of the SAM before the oxidation of the Fc groups.

A close examination of eq 2 reveals that the solution lies in the knowledge of the number of water molecules incorporated into the SAM upon the Fc oxidation. Previous work by Uosaki and co-workers has suggested that water molecules might be incorporated onto the ferrocenylalkanethiol monolayer, as the Fc-terminated SAM becomes more hydrophilic upon Fc oxidation.[56]

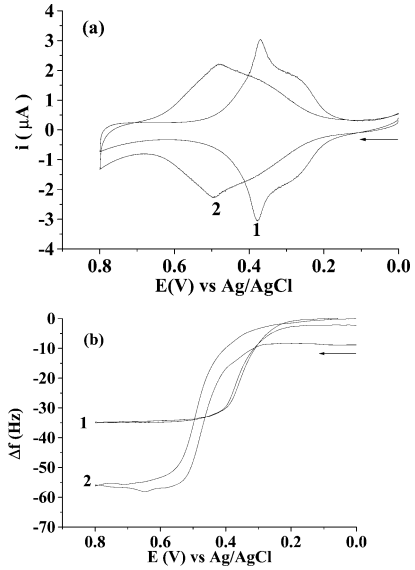

Figure 4. Cyclic voltammograms (panel a) of $FcC_{11}SH$ SAMs in 0.1 M $HClO_4$ (curve 1) and 0.1 M HNO_3 (curve 2) and the corresponding frequency−potential diagrams (panel b). Arrows indicate the scan direction, and the scan rate was 50 mV/s.

The amount of total water loading (including both the water molecules inserted into and residing onto the SAM) can be quantified by EQCM.[28,34,52,55,57−59,72] Figure 4 is an overlay of CVs of $FcC_{11}SH$ (curves 1 and 2 in panel a) acquired from 0.1 M $HClO_4$ and 0.1 M HNO_3 and the corresponding frequency−potential diagrams (panel b). The shapes of the CVs are analogous to those in Figure 2, suggesting that the morphologies of the Au films on the crystals and the SPR substrates are comparable. This is not unexpected since both types of Au films were made with sputter coaters using similar operational conditions. The frequency−potential curves are also sigmoidal, indicating that both EC−SPR and EQCM data reflect different aspects of the molecular reorientation triggered by the Fc oxidation. In theory, once the number of Fc groups oxidized is measured, the cumulative mass of the counteranions positioned on top of the ferrocenium ions can be quantified. However, this cannot account for the total mass change monitored by QCM. In fact, the QCM values are greater than those deduced from the voltammetric experiments. This is consistent with findings by Uosaki and co-workers and De Long and Buttry who have attributed such a discrepancy to the water ingression/egression processes.[28,52,59] We obtained values of N_w/N_q (the term coined by Uosaki and co-workers to represent the water molecules per counteranion attached to the monolayer[58]) and listed them in Table 1. Uosaki and co-workers found that 15 molecules could be brought to the $FcC_{11}SH$ monolayer upon the formation of one ferrocenium/perchlorate ion pair. Our EQCM measurements are consistent with the value reported by these researchers. The fact that ClO_4^- is associated with a smaller amount of water is consistent with other studies employing perchloric acid or perchlorate salts as the supporting electrolyte.[52,60] De Long and Buttry have stated that ClO_4^- causes the alkanethiol SAMs bearing redox-active terminal groups to be more compact and to contain fewer solvent molecules than other ions such as Cl^- and NO_3^-.[52] Since nitrate ions are less strongly associated with the ferrocenium cations, a thicker layer of water may be involved during the ion-pair formation. Consequently, the extent of water loading sensed by EQCM is greater.

Although the total number of water molecules brought onto and into the SAM can be measured, we can only estimate the maximum number of water molecules that can be accommodated by the free volume within the alkyl chains. The projected area per $FcC_{11}SH$ adsorbate is calculated from the surface coverage to be 43.5 $Å^2$ and 45.4 $Å^2$ for $HClO_4$ and HNO_3, respectively, and that of a densely packed monolayer of alkyl chains is 21.4 $Å^2$.[1] Thus the maximum area available for water incorporation is the difference (i.e., 22.1 $Å^2$ from $HClO_4$ and 24.0 $Å^2$ from HNO_3). The vertical distance between the sulfur atom and the Fc group is about 17.8 Å (calculated by using 20.0 Å as the chain length of $CH_3(CH_2)_{10}SH$ and 27° as the tilt angle[79]). Thus, the free volumes within the alkyl chains can be estimated to be 393 $Å^3$ ($HClO_4$) and 427 $Å^3$ (HNO_3). Based on the volume of a single water molecule (33.5 $Å^3$), it appears that the maximum numbers of water molecules that can occupy the free volumes are about 12 and 13 for $HClO_4$ and HNO_3, respectively. Since both numbers are smaller than the total number of water molecules per ion pair listed in Table 1, it is evident that EQCM measurements are quite reasonable. In $HClO_4$, the data suggest that 12 out of the 17 water molecules brought to the Fc-terminated SAM upon the Fc oxidation could reside between the alkyl chains (or inside the film), whereas the fraction of water molecules that may enter the film from the HNO_3 solution is much smaller.

Substituting the maximum number of water molecules that is allowed by the free volume of $FcC_{11}SH$ SAM into eq 2, the following relationships between $\Delta\theta$ and Δd can be obtained: $\Delta\theta = -0.216\ \Delta d$ (ClO_4^-) and $\Delta\theta = -0.235\ \Delta d$ (NO_3^-). Finally, the monolayer thickness change for each case can be computed according to the corresponding SPR dip shift (Table 1). These results suggest that hydration of the $FcC_{11}SH$ SAMs could attenuate the redox-induced orientation change, a point that has not been noted before.

As contrasted in Figure 1, it is clear that different monolayer thickness variations will be expected from the two mechanims. In the first mechanism, by assuming the commonly accepted tilt angle of 27° for an alkanethiol SAM, the maximum monolayer thickness change would be $(1 - \cos 27°) \times d \approx 0.3$ nm, which is in good agreement with that reported by Ohtsuka et al.[59] But these authors took into account the diameter of the electrolyte ion, which is greater than the thickness change of the film. As for the second mechanism, the change in the height of the ferrocenylalkanethiol SAM occurs solely at the terminal. The maximum change would be from the configuration wherein the two Cp rings of the Fc molecule are parallel to the electrode to the configuration wherein the rings are perpendicular to the electrode. Since the distance between the two Cp rings is 3.315 Å and the ring diameter is 3.9 Å,[53] the maximum thickness change would be 0.585 Å or 0.0585 nm, if the Fc molecule were flipped. Because Δd values measured in both $HClO_4$ and HNO_3 solutions are greater than 0.0585 nm, flipping the Cp rings cannot be the only process accompanying the redox reaction of the Fc-terminated SAM. Thus, while it is possible that both mechanisms depicted in Figure 1 are responsible for the observed film thickness change, the first mechanism appears to be more important. Such a contention was also suggested by the recent work of Luk and Abbott who studied the switching of liquid crystals initiated by the redox reactions of the Fc-terminated SAMs.[20] Moreover, in both electrolyte solutions, changes in the alkyl chain tilt angles appear to be quite small. Assuming that the first scheme is the sole process given rise by the Fc oxidation reaction, a 0.09 nm thickness change (in $HClO_4$) and a 0.08 nm change (in HNO_3) would correspond to only 2.7° and 2.1° changes of the alkyl chain tilt angles, respectively. Thus, our SPR experiments afforded the first accurate measurements of the maximum changes in the thickness

of Fc-terminated SAMs and provided an assessment of the possible mechanism(s) that may account for the redox-induced orientation change(s).

4. Conclusion

EC−SPR and EQCM were employed in tandem to study the redox-induced orientation change of $FcC_{11}SH$ SAM in two electrolyte solutions. The high-resolution SPR instrument allowed the SPR dip shift, which is a collective effect of the redox-induced orientation change and the refractive index variation, to be determined. The EQCM results confirmed previous reports about the formation of the ferrocenium/counteranion pair and loading of water molecules onto and into the SAM. The extent of water loading is greater than that allowed by the free volume between the alkyl chains, suggesting that not all of the water molecules are incorporated into the SAM. The maximum thickness changes of the $FcC_{11}SH$ SAM in 0.1 M $HClO_4$ and 0.1 M HNO_3 were deduced to be 0.09 and 0.08 nm, respectively, assuming that the void space between the alkyl chains is completely filled with water molecules. Such small changes have two important implications: (1) the two mechanisms concerning the redox-induced orientation change, viz., the decrease of the tilt angle of the alkyl chain with respect to the surface normal and the rotation of the Cp rings around the Fc-C chain, both appear to be plausible, and (2) if the predominant process were the swinging of the tilt angle of the alkyl chain, the magnitudes of such changes would not be significant. Even if all the void space were assumed to be occupied by water molecules brought into the SAM by the redox process and Cp rings remained stationary, the maximum changes of the tilt angles would be only 2.7° in $HClO_4$ and 2.1° in HNO_3. Our work demonstrated that EC−SPR is a powerful technique for measuring conformational or film thickness changes that are as small as a fraction of the length of a chemical bond. Moreover, the tandem use of EC−SPR and EQCM enables one to study different aspects of the redox-induced film thickness changes, ion-pair formation, and hydration.

Acknowledgment. This work was supported by grants from the Chinese Academy of Sciences (One Hundred Persons Award) and the National Natural Science Foundation (Grant No. 20225517). We also thank Dr. Fayi Song and Mr. Yi Xue for their technical assistance and helpful discussions.

References and Notes

(1) Laibinis, P. E.; Bain, C. D.; Nuzzo, R. G.; Whitesides, G. M. *J. Phys. Chem.* **1995**, *99*, 7663−7676.
(2) Sinniah, K.; Cheng, J.; Terrettaz, S.; Reutt-Robey, J. E.; Miller, C. J. *J. Phys. Chem.* **1995**, *99*, 14500−14505.
(3) Hou, Y. C.; Chen, Y. S.; Amro, N. A.; Wadu-Mesthrige, K.; Andreana, P. R.; Liu, G. Y.; Wang, P. G. *Chem. Commun.* **2000**, 1831−1832.
(4) Lopez, G. P.; Biebuyck, H. A.; Harter, R.; Kumar, A.; Whitesides, G. M. *J. Am. Chem. Soc.* **1993**, *115*, 10774−10781.
(5) Yu, H. Z.; Ye, S.; Zhang, H. L.; Uosaki, K.; Liu, Z. F. *Langmuir* **2000**, *16*, 6948−6954.
(6) Buda, M.; Ion, A.; Moutet, J. C.; Saint-Aman, E.; Ziessel, R. *J. Electroanal. Chem.* **1999**, *469*, 132−138.
(7) He, Z. L.; Bhattacharyya, S.; Cleland, W. E., Jr.; Hussey, C. L. *J. Electroanal. Chem.* **1995**, *397*, 305−310.
(8) Kondo, T.; Horiuchi, S.; Yagi, I.; Ye, S.; Uosaki, K. *J. Am. Chem. Soc.* **1999**, *121*, 391−398.
(9) Leavy, M. C.; Bhattacharyya, S.; Cleland, W. E.; Hussey, C. L. *Langmuir* **1999**, *15*, 6582−6586.
(10) Kang, X. F.; Jin, Y. D.; Cheng, G. J.; Dong, S. J. *Langmuir* **2002**, *18*, 1713−1718.
(11) Lexa, D.; Saveant, J. M. *J. Am. Chem. Soc.* **1977**, *100*, 3222−3223.
(12) Aydogan, N.; Abbott, N. L. *Langmuir* **2001**, *17*, 5703−5706.
(13) Xie, T.; Liang, Y. M.; Liu, W. Y.; Li, B. J.; Ma, Y. X. *Chem. Commun.* **2001**, *17*, 1578−1579.
(14) Kondo, T.; Takechi, M.; Sato, Y.; Uosaki, K. *J. Electroanal. Chem.* **1995**, *381*, 203−209.
(15) Uosoki, K.; Sato, Y.; Kita, H. *Electrochim. Acta* **1991**, *36*, 1793−1798.
(16) Collard, D. M.; Fox, M. A. *Langmuir* **1991**, *7*, 1192−1197.
(17) Krysinski, P.; Moncelli, M. R.; Tadini-Buoninsegni, F. *Electrochim. Acta* **2000**, *45*, 1885−1892.
(18) Aoki, K.; Kakiuchi, T. *J. Electroanal. Chem.* **1998**, *452*, 187−192.
(19) Brevnov, D. A.; Finklea, H. O.; Ryswyk, H. V. *J. Electroanal. Chem.* **2001**, *500*, 100−107.
(20) Luk, Y.; Abbott, N. L. *Science* **2003**, *301*, 623−626.
(21) Imahort, H.; Norieda, H.; Ozawa, S.; Ushida, K.; Yamada, H.; Azuma, T.; Tamaki, K.; Sakata, Y. *Langmuir* **1998**, *14*, 5335−5338.
(22) Willman, K. W.; Rocklin, R. D.; Nowak, R.; Kuo, K. N.; Schultz, F. A.; Murray, R. W. *J. Am. Chem. Soc.* **1980**, *102*, 7629−7634.
(23) Badia, A.; Carlini, R.; Fernandz, A.; Battaglini, F.; Mikkelsen, S. R.; English, A. M. *J. Am. Chem. Soc.* **1993**, *115*, 7053−7060.
(24) Creager, S. E.; Rowe, G. K. *Anal. Chim. Acta* **1991**, *246*, 233−239.
(25) Creager, S. E.; Rowe, G. K. *J. Electroanal. Chem.* **1994**, *370*, 203−211.
(26) Creager, S. E.; Rowe, G. K. *J. Electroanal. Chem.* **1997**, *420*, 291−299.
(27) Chidsey, C. E. D.; Bertozzi, C. R.; Putvinski, T. M.; Mujsce, A. M. *J. Am. Chem. Soc.* **1990**, *112*, 4301−4306.
(28) De Long, H. C.; Donohue, J. J.; Buttry, D. A. *Langmuir* **1991**, *7*, 2196−2202.
(29) Green, J. B. D.; Mcdermott, M. T.; Porter, M. D. *J. Phys. Chem.* **1996**, *100*, 13342−13345.
(30) Guo, L. H.; Facci, J. S.; Mclendon, G. *J. Phys. Chem.* **1995**, *99*, 8458−8461.
(31) Murgida, D. H.; Hildebrandt, P. *J. Mol. Struct.* **2001**, *565−566*, 97−100.
(32) Napper, A. M.; Liu, H. Y.; Waldeck, D. H. *J. Phys. Chem. B* **2001**, *105*, 7699−7707.
(33) Porter, M. D.; Bright, T. B.; Allara, D. L.; Chidsey, C. E. D. *J. Am. Chem. Soc.* **1987**, *109*, 3559−3568.
(34) Rowe, G. K.; Creager, S. E. *Langmuir* **1991**, *7*, 2307−2312.
(35) Sabapathy, R. C.; Bhattacharyya, S.; Leavy, M. C.; Cleland, W. E., Jr.; Hussey, C. L. *Langmuir* **1998**, *14*, 124−136.
(36) Sek, S.; Palys, B.; Bilewicz, R. *J. Phys. Chem. B* **2002**, *106*, 5907−5914.
(37) Smalley, J. F.; Feldberg, S. W.; Chidsey, C. E. D.; Linford, M. R.; Newton, M. D.; Liu, Y. P. *J. Phys. Chem.* **1995**, *99*, 13141−13149.
(38) Sumner, J. J.; Creager, S. E. *J. Am. Chem. Soc.* **2000**, *122*, 11914−11920.
(39) Sumner, J. J.; Creager, S. E. *J. Phys. Chem. B* **2001**, *105*, 8739−8745.
(40) Bhushan, B.; Liu, H. *Phys. Rev. B* **2001**, *63*, 245412.
(41) Gooding, J. J.; Hibbert, D. B. *Trends Anal. Chem.* **1999**, *18*, 525−533.
(42) Kerman, K.; Ozkan, D.; Kara, P.; Meric, B.; Gooding, J. J.; Ozsoz, M. *Anal. Chim. Acta* **2002**, *462*, 39−47.
(43) Patel, N.; Davies, M. C.; Hartshorne, M.; Heaton, R. J.; Roberts, C. J.; Tendler, S. J. B.; Williams, P. M. *Langmuir* **1997**, *13*, 6485−6490.
(44) Ozkan, D.; Erdem, A.; Kara, P.; Kerman, K.; Gooding, J. J.; Nielsen, P. E.; Ozsoz, M. *Electrochem. Commun.* **2002**, *4*, 796−802.
(45) Huang, E.; Zhou, F.; Deng, L. *Langmuir* **2000**, *16*, 3272−3280.
(46) Millan, K. M.; Mikkelsen, S. R. *Anal. Chem.* **1993**, *65*, 2317−2323.
(47) Frey, B. L.; Corn, R. M. *Anal. Chem.* **1996**, *68*, 3187−3193.
(48) Offord, D. A.; Sachs, S. B.; Ennis, M. S.; Eberspacher, T. A.; Griffin, J. H.; Chidsey, C. E. D.; Collman, J. P. *J. Am. Chem. Soc.* **1998**, *120*, 4478−4487.
(49) Dong, S. J.; Li, J. H. *Bioelectrochem. Bioenerg.* **1997**, *42*, 7−13.
(50) Dong, X.; Lu, J.; Cha, C. *Bioelectrochem. Bioenerg.* **1997**, *42*, 63−69.
(51) Qian, Z.; Shi, X.; Zhuang, J.; Kong, J.; Deng, J. *Bioelectrochem. Bioenerg.* **1998**, *46*, 193−198.
(52) De Long, H. C.; Buttry, D. A. *Langmuir* **1990**, *6*, 1319−1322.
(53) Viana, A. S.; Jones, A. H.; Abrantes, L. M.; Kalaji, M. *J. Electroanal. Chem.* **2001**, *500*, 290−298.
(54) Viana, A., S.; Abrantes, L. M.; Jin, G.; Floate, S.; Nichols, R. J.; Kalaji, M. *Phys. Chem. Chem. Phys.* **2001**, *3*, 3411−3419.
(55) Ye, S.; Sato, Y.; Uosaki, K. *Langmuir* **1997**, *13*, 3157−3161.
(56) Ye, S.; Haba, T.; Sato, Y.; Shimazu, K.; Uosaki, K. *Phys. Chem. Chem. Phys.* **1999**, *1*, 3653−3659.
(57) Uosaki, K.; Sato, Y.; Kita, H. *Langmuir* **1991**, *7*, 1511−1514.
(58) Shimazu, K.; Yagi, I.; Sato, Y.; Uosaki, K. *J. Electroanal. Chem.* **1994**, *372*, 117−124.

(59) Shimazu, K.; Yagi, I.; Sato, Y.; Uosaki, K. *Langmuir* **1992**, *8*, 1385−1387.
(60) Ohtsuka, T.; Sato, Y.; Uosaki, K. *Langmuir* **1994**, *10*, 3658−3662.
(61) Xia, C.; Advincula, R. C.; Baba, A.; Knoll, W. *Langmuir* **2002**, *18*, 3555−3560.
(62) Baba, A.; Advincula, R. C.; Knoll, W. *Stud. Interface Sci.* **2001**, *11*, 55−70.
(63) Baba, A.; Park, M.-K.; Advincula, R. C.; Knoll, W. *Langmuir* **2002**, *18*, 4648−4652.
(64) Hanken, D. G.; Jordan, B. L. F.; Corn, R. M. In *Electroanalytical Chemistry*; Rubinstein, I., Ed.; M. Dekker: New York, 1998; Vol. 20.
(65) Tao, N. J.; Boussaad, S.; Huang, W. L.; Arechabaleta, R. A.; D'Agness, J. *Rev. Sci. Instrum.* **1999**, *70*, 4656−4660.
(66) Boussaad, S.; Pean, J.; Tao, N. J. *Anal. Chem.* **2000**, *72*, 222−226.
(67) Song, F.; Zhou, F.; Wang, J.; Tao, N.; Lin, J.; Vellanoweth, R.; Morquecho, Y.; Wheeler-Laidman, J. *Nucleic Acids Res.* **2002**, *30*, e72.
(68) Plunkett, M. P.; Wang, Z.; Rutland, M. W.; Johannsmann, D. *Langmuir* **2003**.
(69) Briseno, A. L.; Song, F. Y.; Baca, A. J.; Zhou, F. *J. Electroanal. Chem.* **2001**, *513*, 16−24.
(70) Kolomenskii, A. A.; Gershon, P. D.; Schuessler, H. A. *Appl. Optics* **1997**, *36*, 6539−6547.
(71) Chidsey, C. E. D.; Loiacono, D. N. *Langmuir* **1990**, *6*, 682−691.
(72) Sato, Y.; Mizutani, F.; Shimazu, K.; Ye, S.; Uosaki, K. *J. Electroanal. Chem.* **1999**, *474*, 94−99.
(73) Deakin, M. R.; Buttry, D. A. *Anal. Chem.* **1989**, *61*, 1147A−1154A.
(74) Schneider, T. W.; Buttry, D. A. *J. Am. Chem. Soc.* **1993**, *115*, 12391−12397.
(75) Ju, H. X.; Leech, D. *Phys. Chem. Chem. Phys.* **1999**, *1*, 1549−1554.
(76) Bard, A. J.; Faulkner, L. R. *Electrochemical Methods: Fundamentals and Applications*; John Wiley & Sons: New York, 2001.
(77) Popenoe, D. D.; Deinhammer, R. S.; Porter, M. D. *Langmuir* **1992**, *8*, 2521−2530.
(78) *Handbook of Analytical Chemistry*; Chemical Industry Press: Beijing, 1997; Vol. 1.
(79) Ulman, A. *An Introduction to Ultrathin Organic Films: From Langmuir−Blodgett to Self-Assembly*; Academic Press: Boston, 1991.